Available online at www.sciencedirect.com
SCIENCE DIRECT®
Journal of Catalysis 219 (2003) 404–416
JOURNAL OF CATALYSIS
www.elsevier.com/locate/jcat

The influence of dissolved gases on the adsorption of cinchonidine from solution onto Pt surfaces: an in situ infrared study

Zhen Ma, Jun Kubota, and Francisco Zaera *

Department of Chemistry, University of California, Riverside, CA 92521, USA

Received 3 March 2003; revised 7 May 2003; accepted 14 May 2003

Abstract

The influence of different dissolved gases on the adsorption of cinchonidine from CCl_4 solutions onto polycrystalline platinum surfaces has been studied by in situ reflection–absorption infrared spectroscopy (RAIRS). It was observed that Ar, N_2, O_2, air, or CO_2 neither enhances the adsorption of cinchonidine nor damages cinchonidine adlayers once they have formed on the surface. On the other hand, H_2 plays a unique role, initially facilitating the uptake of cinchonidine, but later removing some of the resulting adsorbed cinchonidine from the platinum surface. It was also found that CO is a strong inhibitor, significantly retarding the adsorption of cinchonidine. Adsorbed CO can be removed by H_2 dissolved in the cinchonidine solution, a process that also boosts the adsorption of cinchonidine. O_2 can remove the surface adsorbed CO as well, but without facilitating cinchonidine adsorption. The cleanliness of Pt surfaces at different stages of the experiment was probed by CO adsorption. Possible correlations between the RAIRS results from the present study and reported data from catalytic studies are discussed.

Keywords: Enantioselective hydrogenation; Chiral modifier; Cinchonidine; Adsorption; Platinum; Reflection–absorption infrared spectroscopy

1. Introduction

Asymmetric catalysis plays a key role in the manufacture of chiral pharmaceuticals, agrochemicals, flavors, and other important intermediates for chemical industries [1]. Most of the enantioselective syntheses carried out nowadays in industrial settings rely on the use of homogeneous catalysts, mostly chiral metal complexes [2]. However, if available, heterogeneous enantioselective catalysts would be preferred, because they offer some inherent advantages related to separation, handling, stability, recovery, and re-use [3]. One of the most promising strategies to fabricate enantioselective heterogeneous catalysts is to adsorb a chiral modifier onto a catalytically active metal surface. However, although numerous heterogeneous systems using this strategy have been explored to date, only two, tartaric acid-modified nickel [4–6] and cinchona-modified platinum [6–12], have proven successful. Unfortunately, these two families of catalysts have so far shown to be of limited usefulness, being effective mainly for the enantioselective hydrogenation of β- and α-ketoesters, respectively. Moreover, their performance has proven highly sensitive to slight variations in the nature of the reactant, the structure of the modifier, the preparation of the catalyst, or the conditions of the reaction [3,10,11]. At present, there is still no sufficient understanding of the reasons underlying this behavior.

In an attempt to address the lack of molecular-level understanding of this heterogeneous chiral catalysis, the characterization of chiral modifiers on surfaces has been studied recently with a number of surface-sensitive techniques [13]. For instance, the interaction of 10,11-dihydrocinchonidine with Pt(111) has been investigated by X-ray photoelectron spectroscopy (XPS), ultraviolet photoelectron spectroscopy (UPS), low-energy electron diffraction (LEED) [14,15], and near-edge X-ray absorption fine structure (NEXAFS) [16], and the adsorption of naphthylethylamine and lepidine on Pt surfaces has also been monitored by NEXAFS [17,18]. The findings from those studies have certainly furnished deeper insights into the basic chemistry of chiral adsorbates on surfaces. However, their extrapolation to chiral catalysis is limited by the fact that most of those experiments have been carried out under ultrahigh vacuum conditions quite different from those encountered in the working catalysts.

* Corresponding author.
E-mail address: francisco.zaera@ucr.edu (F. Zaera).

0021-9517/$ – see front matter
doi:10.1016/S0021-9517(03)00232-X

To our knowledge, there have been only a handful of spectroscopic investigations of these catalytic systems in situ at the solid–liquid interface. In one, the adsorption of cinchonidine from CH_2Cl_2 solutions onto Pt/Al_2O_3 and Pd/Al_2O_3 model catalysts was probed using attenuated total reflective infrared (ATR-IR) spectroscopy [19–21]. It was found that the adsorption mode of cinchonidine is coverage dependent, and that up to three different cinchonidine species can coexist on the surfaces of those catalysts. A correlation between the adsorption geometry of cinchonidine and the enantioselectivity of ethyl pyruvate hydrogenation was also identified by an in situ reflection–absorption infrared spectroscopy (RAIRS) study in our laboratory [22]. More recently, surface enhanced Raman spectroscopy (SERS) has been used to further characterize the properties of adsorbed cinchonidine on Pt from ethanol solutions [23]. In that study, adsorbed cinchonidine was found to be somewhat tilted on the platinum surfaces. These reports all show the great promise of using in situ spectroscopy to advance the molecular-level understanding of how these chiral systems work. Nevertheless, much more work is still needed in this direction. Also, in more general terms, in situ studies of liquid–solid interfaces of catalytic relevance have so far been scarce, and represent one of the frontiers of surface science [24,25].

As mentioned above, the performance of cinchona chiral modifiers in enantioselective hydrogenation catalysis is defined to a great extent by the details of the procedures used for catalyst preparation as well as by the reaction conditions. In particular, it has been shown that gases, either in gas phase or dissolved in the liquid reaction mixture, play an important yet intriguing role in high-temperature prereduction [26–28], ambient temperature pretreatment [29–32], storage [27,33], stability [34,35], and poisoning [36–38] of the Pt catalysts used for hydrogenation of α-ketoesters. Following our previous in situ IR studies on this cinchonidine/platinum system [22,39–41], here we report on our investigation of the effect of different gases on the adsorption of cinchonidine. Evidence is presented below for the beneficial effect of H_2 in facilitating the adsorption of cinchonidine, for the site-blocking effect of O_2, and for the poisoning effect of CO in retarding the cinchonidine adsorption. The removal of adsorbed CO by exposure to solutions with dissolved H_2 and O_2 and their effect on cinchonidine adsorption are also addressed.

2. Experimental

The experimental setup used for our in situ infrared spectroscopy characterization of cinchonidine adsorption from solution onto platinum surfaces is schematically shown in Fig. 1. This arrangement is based on a liquid cell equipped with gas and liquid introduction stages, and a circuit for electrochemical oxidation–reduction cycles (ORCs) to clean the Pt disk used as the model catalyst. The technical details of this cell, together with a number of studies performed to test its performance, have already been reported elsewhere [41]. Briefly, a polycrystalline Pt disk (Goodfellow), 10 mm in diameter and 1 mm in thickness, was polished to a roughness of 0.25 μm by using a series of diamond pastes, and mounted on the front of a supporting rod inserted through the center of the cell. A CaF_2 prism, cut in a trapezoidal shape with two faces beveled to 60°, was placed in front of the Pt sample to let the infrared beam in and out of the cell. The distance between the Pt sample and the prism was controlled by a micrometer attached to the end of the sample rod. Liquid was injected into the approximately 5-cm^3 volume enclosed between the Pt sample rod and a CaF_2 prism (when the sample is retracted) via a small tube attached to the side of the cell. Gases were bubbled at fixed flows into the solution via a gas handling system connected to the inlet tube, and monitored by using bubbling bottles.

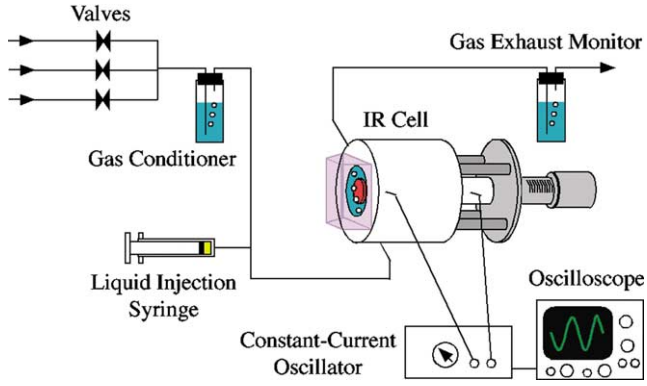

Fig. 1. Schematic representation of the experimental setup used here for the in situ IR characterization of the adsorption of cinchonidine from solutions onto Pt surfaces. The main cell consists of a platinum disk, used as the surface for our adsorption studies, a CaF_2 prism for optical guidance of the IR beam, and a liquid solution trapped between those two elements. The overall arrangement includes gas and liquid sample introduction stages as well as the electronics used for the electrochemical oxidation–reduction cycles needed to preclean the Pt surfaces.

The RAIRS measurements were performed by focusing the IR beam from a Mattson Sirius 100 FTIR spectrometer through a polarizer and the CaF_2 prism onto the Pt surface, and by refocusing the reflected beam into a liquid N_2-cooled mercury–cadmium–telluride (MCT) detector. A grazing incidence angle of 60° into the prism was chosen to avoid total internal reflection at the prism–solution interface [41]. Ratios of p/s polarization spectra were used to discriminate between adsorbed and dissolved species. All the reported spectra are the results of averages from 512 scans, taken with 4 cm^{-1} resolution. It should be mentioned that the IR absorption peaks observed with cinchonidine in our experiments are surprisingly strong, reaching values on the order of 5% transmittance. These large infrared absorption cross sections are apparently associated with solvent effects, since smaller intensities were observed for the adsorbates under vacuum [41]. In any case, a number of experiments were carried out to ensure that the signals are due to monolayer adsorption, not to molecules in solution or condensed in multilayers [41].

The Pt surface was cleaned before each experiment by an electrochemical treatment that uses two electrodes, the Pt disk and a Pt wire placed inside the cell. A 0.1 M $KClO_4$ aqueous solution (the supporting electrolyte) was injected into the cell, and the electrodes were connected to a constant-current oscillator set to a sample current at 15 mA to carry out repeating ORCs for 1.0 h. During this ORC treatment, H_2 was bubbled continuously into the cell to remove any O_2 dissolved in the solution. After cleaning of the Pt surface, the $KClO_4$ solution was replaced with pure CCl_4, the Pt sample was pressed tightly against the prism to form a thin (ca. 2–10 μm) liquid film above the surface, and two reference IR spectra were recorded, with p- and s-polarized light, respectively. The Pt disk was then pulled back again, the pure CCl_4 replaced by a cinchonidine/CCl_4 solution, and a specific gas bubbled into the cell at a flow rate of 0.85 cm^3/min for a specified time. The Pt disk was kept in the retracted position throughout the gas bubbling to allow for fast saturation of the liquid with the gas in the region immediately above the surface. Nevertheless, transport effects could not be completely eliminated: it took on the order of 10 min to induce a complete change in the nature of the surface adsorbed layer in the fastest cases studied here, and differences in rates for the adsorption processes were seen when the gas flow was varied. Finally, the Pt disk was pressed one more time against the prism, and new p- and s-polarized spectra were recorded. The resulting p/s ratio spectra from the cinchonidine/CCl_4 sample were divided by the equivalent background traces obtained for the pure CCl_4 (the reference data mentioned above).

Cinchonidine (96%) and CCl_4 (99.9%) were purchased from Aldrich, and used as received. Cinchonidine solutions of 3.4 mM were prepared by ultrasonic treatment of cinchonidine/CCl_4 slurries for 0.5–1.0 h followed by cooling down to room temperature and filtering of any traces of undissolved cinchona residue. CO (99.5%), Ar (99.999%), O_2 (99.99%), and CO_2 (99.99%) were purchased from Matheson, and H_2 (99.999%) and N_2 (99.99%) from Liquid Carbonic, and all were used as supplied.

3. Results

3.1. General considerations and role of H_2

It has been empirically realized that hydrogen pretreatments at high temperatures are necessary for the optimal performance of supported Pt catalysts in enantioselective hydrogenations, presumably to ensure the complete reduction of the metal and the removal of contaminants from the surface [26–28]. Sometimes the Pt catalysts are also briefly preactivated with H_2 dissolved in the solvent before the reaction is carried out [12,32–35]. In our recent spectroscopic studies on the adsorption geometry of cinchonidine on Pt it was noted that, indeed, it seem to be necessary either to use H_2 presaturated solutions [19–21] or to bubble H_2 in situ through the solution [22] to aid with the adsorption of cinchonidine from solution onto the Pt surface. Here we report on a systematic study carried out to better understand the role of dissolved H_2 and other gases in this system.

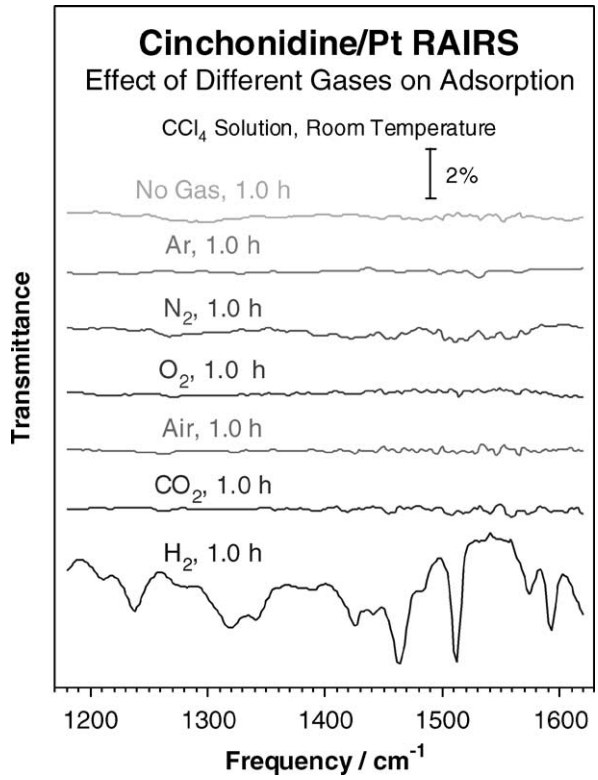

Fig. 2. In situ reflection–absorption infrared spectroscopy (RAIRS) data illustrating the effect of different dissolved gases (Ar, N_2, O_2, air, CO_2, and H_2) on the adsorption of cinchonidine onto a Pt disk from a CCl_4 solution. The spectra were obtained by individual experiments in which cinchonidine solutions were injected into the IR cell and the specified gases were bubbled for 1.0 h. The data in this figure point to the unique role of dissolved H_2 in facilitating the adsorption of cinchonidine.

Fig. 2 summarizes typical results from our in situ IR characterization of cinchonidine adsorption on platinum as a function of surface pretreatment with different gases. These data indicate that no significant amount of cinchonidine adsorbs directly from cinchonidine solutions onto the surface when no gases are bubbled through those solutions. Similarly, cinchonidine adsorption is only marginally detected when Ar, N_2, O_2, air, or CO_2 is bubbled into the solution. Only by bubbling H_2 it is possible to see the development of the IR absorption signals about 1236, 1319, 1342, 1425, 1441, 1463, 1512, 1574, and 1593 cm^{-1} indicative of cinchonidine adsorption [20,22]. Clearly, H_2 is unique in facilitating the adsorption of cinchonidine on Pt.

A number of additional gas-switching experiments were conducted to complement the information obtained by the studies described above. Since similar behavior was observed with all the gases (Ar, N_2, O_2, air, CO_2) used in this study, only the results for O_2 are shown in Fig. 3. Almost no cinchonidine adsorption is observed after the Pt surface is pretreated in situ with Ar, N_2, O_2, air, or CO_2.

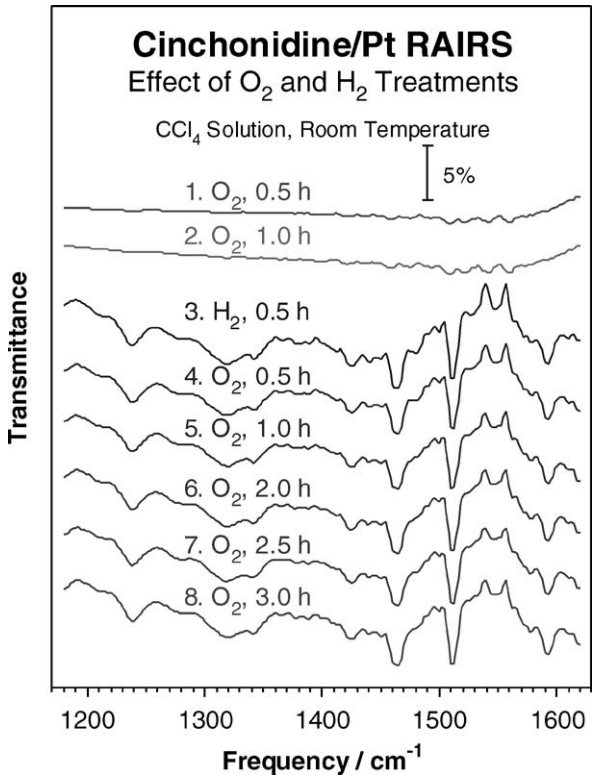

Fig. 3. RAIRS results from experiments on cinchonidine adsorption from a CCl_4 solution where the bubbling gas was switched from O_2 to H_2 and then back to O_2. It is seen here that H_2 efficiently facilitates the adsorption of cinchonidine on O_2-preexposed surfaces, and that adsorption is quite strong and not affected in any significant way by further O_2 exposures at room temperature. Similar trends were observed in experiments with Ar, N_2, air, and CO_2.

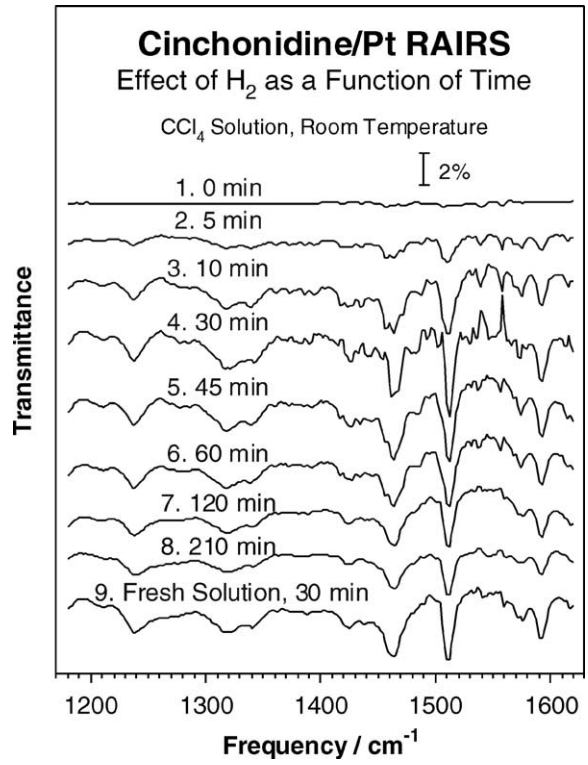

Fig. 4. Effect of bubbling H_2 on adsorbed cinchonidine on Pt as a function of time. Three phenomena can be extracted from this figure: (1) a transient period before the maximum adsorption of cinchonidine is reached, presumably due to gradual cleaning of the Pt surface by the dissolved H_2 in solution; (2) a gradual disappearance of the adsorbed cinchonidine layer after the initial 30 min of H_2 treatment, the results of hydrogenation of adsorbed cinchonidine by H_2; and (3) the renewal of the saturated cinchonidine surface after switching to a fresh cinchonidine solution.

On the other hand, obvious IR peaks due to adsorbed cinchonidine are easily detected after only 0.5 h following the switching to H_2 regardless of the treatment of the Pt sample used beforehand, in particular the preexposure to the other gases. Moreover, once the cinchonidine has been deposited on the surface, no significant deterioration of the adsorbed layer is observed even after 2.0- to 3.0-h exposures back to those original gases. In particular, Fig. 3 shows that O_2 cannot remove the cinchonidine adsorbed on metallic Pt sites, although it appears that cinchonidine adsorption is not possible on preoxidized (O_2 pretreated) Pt sites. The fact that cinchonidine, once adsorbed from a CCl_4 solution, cannot be removed from the surface by switching from H_2 to other gases (nor can it be readily flushed away by pure CCl_4 [42]), indicates that its adsorption is quite strong under our experimental conditions.

The effect of H_2 exposure on cinchonidine adsorption as a function of time was investigated next. Fig. 4 displays a set of IR spectra obtained as a function of H_2 bubbling time. It can be seen there that cinchonidine adsorption is already apparent after H_2 exposures as short as 5 min, but continues until reaching a maximum coverage after a 30-min H_2 treatment. The IR band intensities then decrease gradually after longer H_2 bubbling times, probably because of the slow hydrogenation of the chiral modifier on the Pt catalyst [34,35, 43–45]; they decrease to approximately half of their maximum values after bubbling H_2 for 210 min. However, once a fresh cinchonidine solution is introduced into the IR cell and H_2 is again bubbled for 30 min, the earlier cinchonidine-saturated surface is completely regenerated. It is interesting to note that nowhere in these experiments was evidence obtained for a change in cinchonidine adsorption geometry with varying cinchonidine surface coverage, as we reported before as a function of cinchonidine concentration [22]. We explain this observation by assuming that, as long as gases are bubbled in the liquid solution, the platinum surface is never free of adsorbates: a competition between cinchonidine and other potential adsorbates for surface sites ensures that the platinum surface always stays saturated. This competitive adsorption may play a particularly important role in determining the behavior seen when oxygen and carbon monoxide are added to the mixtures (see below).

3.2. Surface characterization and role of CO adsorption

The results reported above indicate that hydrogen treatments efficiently facilitate the adsorption of cinchonidine on Pt surfaces, an empirical phenomenon also noted by oth-

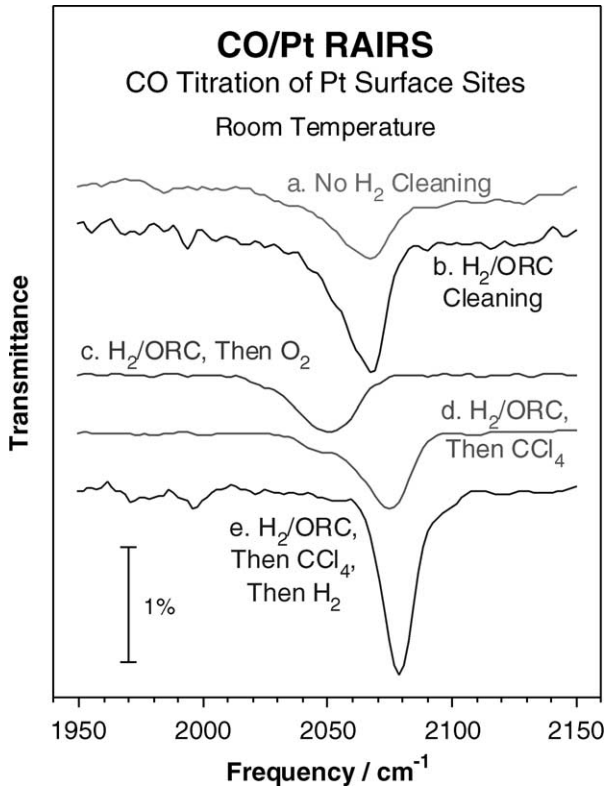

Fig. 5. CO titration RAIRS data from Pt surfaces after different treatments: (a) after polishing and ultrasonic washing in ethanol and H_2O; (b) after oxidation–reduction cycles (ORCs) in a $KClO_4$ solution with H_2 bubbling; (c) after H_2/ORC cleaning followed by exposure to dissolved O_2 for 1.0 h; (d) after H_2/ORC treatment followed by rinsing with CCl_4; and (e) after H_2/ORC cleaning, CCl_4 rinsing, and renewed H_2 bubbling for 1.0 h. These results highlight the need for H_2 treatments to prepare clean Pt surfaces for cinchonidine adsorption.

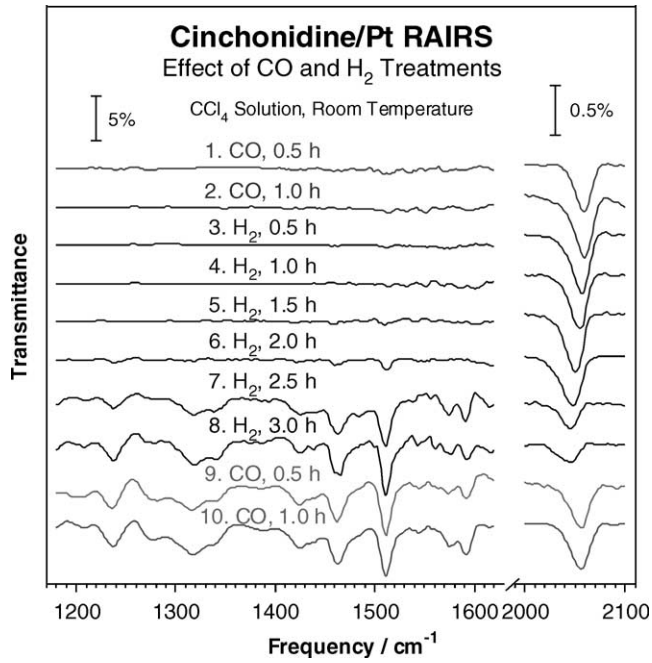

Fig. 6. RAIRS results from a gas-switching experiment from CO to H_2 and then back to CO. The data clearly show the retardation effect that adsorbed CO exerts on cinchonidine adsorption. Red shifts in the C–O stretching frequency and decreases in the CO coverage are also seen after subsequent exposures to H_2-saturated cinchonidine solutions, and limited CO readsorption is also observed after saturation of the surface with cinchonidine. This figure points to the poisoning effect of CO on cinchonidine adsorption, the synergistic effect of H_2 and cinchonidine on the removal of adsorbed CO, and the availability of empty sites on cinchonidine-covered surfaces.

ers [20]. To account for such a promoting effect, the availability of adsorption sites on the Pt surface after each of the different steps in a typical cinchonidine adsorption experiment was probed by a number of CO titration experiments. Typical results from those experiments, carried out by IR measurements after exposing the Pt surfaces with different pretreatment to CO for 1.0 h, are summarized in Fig. 5.

In terms of the C–O stretching IR band seen in the spectra in Fig. 5, it was found that

(1) if the Pt substrate is exposed to CO after no pretreatment other than ultrasonic cleaning of the freshly polished surface, only a low surface coverage, 30–40% of saturation, is observed (top trace);
(2) the cleanliness of the surface is significantly enhanced after either electrochemical ORCs in the presence of H_2 (second trace from top) or after in situ H_2 pretreatment in $KClO_4$ solutions (without ORCs, not shown);
(3) right after the electrochemical pretreatment, if bubbling H_2 is switched to O_2 or air for 1.0 h, the availability of adsorption sites for CO is reduced back to 30–40% of saturation (middle trace);
(4) if either a cinchonidine solution or the pure CCl_4 solvent is injected right after the electrochemical pretreatment, the adsorption of CO is again limited to near half-saturation (second from bottom); and
(5) if the Pt disk is cleaned again by bubbling H_2 for 0.5–1.0 h, after the injection of the CCl_4 solvent on precleaned Pt, complete cleanliness of the surface is restored (bottom trace).

All of these results are congruent with the facilitating effect of H_2 toward cinchonidine adsorption manifested by the data in Figs. 2, 3, and 4.

The direct role of CO in controlling the adsorption of cinchonidine deserves special mention, because that species proved to be a particularly strong inhibitor for cinchonidine uptake. In the experiment illustrated in Fig. 6, CO was first bubbled into a cell filled with cinchonidine solution for up to 1.0 h (top two traces). During that time, significant CO adsorption was manifested by a strong CO IR peak around 2060 cm^{-1} due to carbon monoxide linearly coordinated to the Pt metal, but only a small amount of coadsorbed cinchonidine is observed. Next, the gas was switched from CO to H_2. At that point, as opposed to what was seen with the predosing of other gases (Fig. 3), no obvious immediate (within 0.5 h) adsorption of cinchonidine was detected. Instead, the IR signal from adsorbed cinchonidine starts to

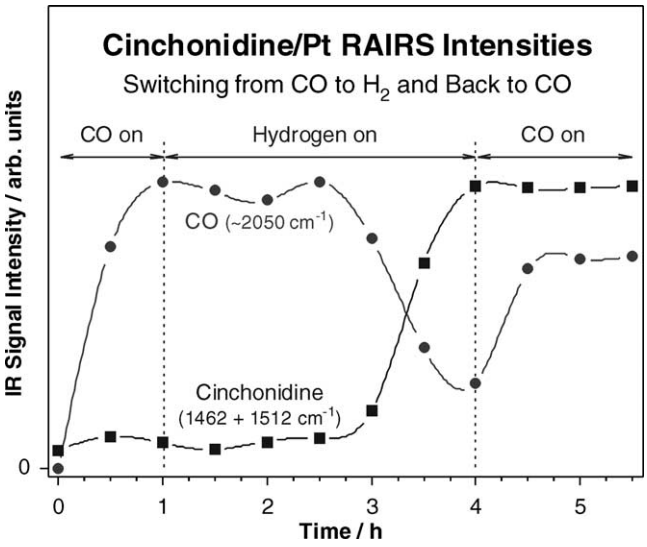

Fig. 7. Correlation between the IR peak intensities of the linearly bonded CO at 2044–2060 cm^{-1} (●) and those of cinchonidine at 1462 and 1512 cm^{-1} (■) in the CO–H_2–CO switching experiments reported in Fig. 6. During the first CO exposure, only the IR signal intensity for the CO peak grows, and cinchonidine adsorption is negligible. On switching to H_2, the adsorbed CO remains on the surface for approximately 1.5 h, after which significant and rapid CO desorption is accompanied by an enhanced uptake of cinchonidine on the surface. Switching back to CO leads to the readsorption of some CO, but without affecting the cinchonidine adlayer.

be observable only after H_2 bubbling for 1.5–2.0 h, and it reaches a plateau after about 3.0 h (a period of time clearly outside our experimental error due to gas mass transport limitations). The facilitating role of H_2 for cinchonidine adsorption is clearly inhibited by adsorbed CO. It is also of interest to note that during the H_2 bubbling period the position of the linearly bound CO peak shifts gradually, from 2060 to 2050 cm^{-1} in the initial 1.5 h, and that the intensity of that peak is slightly reduced. The CO peak then further shifts to 2044 cm^{-1} and shows a more obvious reduction in intensity after longer H_2 exposure times, indicating a significant decrease in the CO surface coverage. There is a clear correlation between the removal of adsorbed CO and the appearance of cinchonidine surface species, as better seen in the middle section of Fig. 7 (which reports the time evolution of the intensities of representative IR bands for cinchonidine and CO during this experiment). Finally, subsequent switching of the gas from H_2 back to CO does not lead to any noticeable decrease in the intensity of the cinchonidine peaks (at least after 1.5 h of CO treatment), but it does cause the partial growth and blue shift of the IR feature for CO (to 30–35% of the maximum value on the cinchonidine-free clean Pt surface). It appears that cinchonidine adsorption does not completely block all of the Pt sites, and that, even after cinchonidine saturation, there are still some (but not all) Pt sites accessible for further CO adsorption.

To better understand the competition among CO, H_2, and cinchonidine for adsorption sites on the Pt surface, a number of additional experiments were carried out where CO was first bubbled through the IR cell filled with pure CCl_4 (rather than the cinchonidine solution used in the previous experiment), and then switched to H_2. The initial CO coverage on the surface was controlled by the time of exposure of the Pt disk to the CO-bubbling CCl_4. Results from two typical cases, with initial CO coverages below (A) and slightly above (B) that in Fig. 6, are shown in Fig. 8.

As can be seen from Fig. 8B, if CO is bubbled into CCl_4 in the absence of cinchonidine, the CO IR peak grows at 2076 cm^{-1} rather than at 2060 cm^{-1} (as seen in Fig. 6). Note that the CO coverages in Figs. 6 and 8B are approximately equal, so the relative initial red shift ($\Delta\nu = 16\ cm^{-1}$) in Fig. 6 needs to be explained by changes in the nature of the surface caused by the co-adsorption of a small amount of cinchonidine. Similar effects have been previously noted for the co-adsorption of CO with pyridine, benzene, or cinchonidine [38,46]. It is also clear in Fig. 8B that the CO peak red shifts further during the H_2 treatments, by $\Delta\nu = 8\ cm^{-1}$ after 1.0 h and by $\Delta\nu = 11\ cm^{-1}$ after 3.5 h (again an effect reported previously [47]), and that its intensity increases slightly, perhaps because of further adsorption of a small amount of residual CO in the CCl_4 solvent or because of a possible enhancement of the CO IR absorption cross section caused by H_2 [47]. What is clear is that no appreciable loss of CO IR signal is observed upon exposures to H_2 bubbling, indicating that H_2 dissolved in CCl_4 can hardly remove CO adsorbed on cinchonidine-free Pt surfaces, at least at room temperature.

Similar observations are also reported in Fig. 8A for lower initial CO coverages. There it is shown that, when CO is bubbled into a cell filled with CCl_4 for a shorter time, the low CO coverages yield IR peaks centered at lower frequencies. In the example reported here, the initial CO peak intensity is approximately half that in Fig. 8B, and the IR absorption is maximum at 2067 cm^{-1} instead of at 2076 cm^{-1}. The peak intensity increases by about 15% after H_2 bubbling for 0.5 h, the same as before, but then decreases slightly after an additional 3.5 h, as the peak reaches its final position at 2061 cm^{-1}. However, the decrease in CO coverage with H_2 exposure is not as obvious as that shown in Fig. 6B, where cinchonidine was present in the solution, even though the initial CO coverage is obviously lower in the present case. Comparison between Figs. 6 and 8 indicates that a small amount of preadsorbed cinchonidine facilitates the removal of CO in the presence of H_2, and that a synergistic effect between cinchonidine and H_2 toward CO removal is apparent.

3.3. Combined effect of CO and O_2 in cinchonidine adsorption

In another set of gas-switching experiments, the competition between CO and O_2 for adsorption sites in the presence of cinchonidine was tested (Fig. 9). In this case, CO was first bubbled into the cell for 1.0 h, at which point an obvious CO peak at 2064 cm^{-1} was seen in the IR spectrum

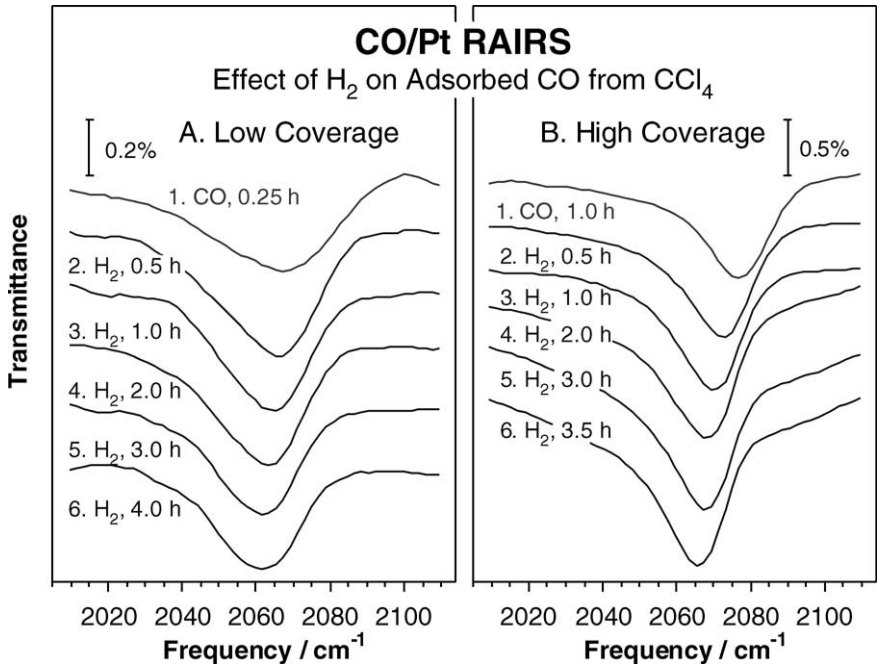

Fig. 8. RAIRS data illustrating the effect of H_2 on CO adsorbed from pure liquid CCl_4. Results are shown here for two different initial CO coverages, obtained by varying the exposure time of the platinum surface to the CO-saturated liquid. Subsequent exposures of those surfaces to dissolved H_2 cause red shifts of the CO IR peak but no significant CO removal, in contrast with the results from the experiments with cinchonidine solutions shown in Fig. 6. The disparity between the two sets of results is most likely related to the role played by the adsorption of a small amount of cinchonidine on the surface. There is a synergistic effect between H_2 and cinchonidine toward the removal of adsorbed CO.

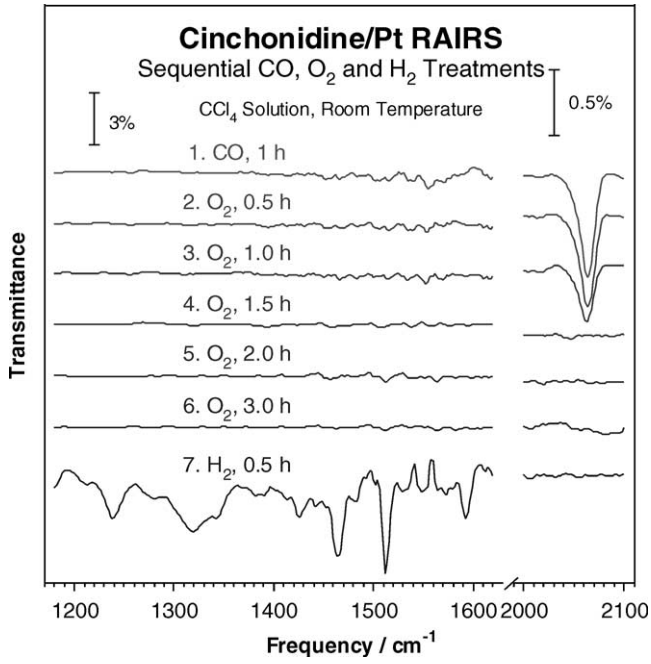

Fig. 9. RAIRS results from a gas-switching experiment from CO to O_2 and then to H_2. O_2 removes the surface-adsorbed CO within 1.5 h of O_2 bubbling, but this does not lead to any appreciable cinchonidine uptake. Only by further treating the Pt surface with H_2 can the cinchonidine be adsorbed to a significant extent. This figure points to the fact that the removal of adsorbed CO does not necessarily lead to the adsorption of cinchonidine, perhaps because of the need for large surface atoms ensemble for the latter.

together with a small amount of cinchonidine (as reported above). Then, on switching from CO to O_2, the IR peak associated with CO decreases in intensity rapidly, and disappears completely after only 1.5 h of O_2 bubbling. However, no surface cinchonidine is adsorbed during this process, in contrast with the behavior illustrated in Fig. 6, where the removal of the adsorbed CO by H_2 is accompanied by the simultaneous adsorption of cinchonidine. Further bubbling of O_2 for up to 3.0 h does not facilitate any cinchonidine uptake. On the other hand, cinchonidine saturation on the Pt surface is possible after 0.5 h following a switch to H_2, as with the exchange from other gases by H_2 (Fig. 3). As a control, a similar experiment was carried out with N_2 instead of O_2. In that case, it was found that N_2 neither facilitates the adsorption of cinchonidine nor causes the reduction of the CO coverage or the shift of the CO peak, not even after 4.0 h (data not shown). It may very well be that the oxidation of adsorbed CO by O_2 at room temperature plays a major role in the removal of CO from the surface in these experiments [48,49].

The CO–O_2 sequence experiments were also carried out in the absence of cinchonidine, with both lower and higher initial CO coverages, as shown in Fig. 10. In both cases it is clear that O_2 can indeed remove the CO adsorbed on the surface, but, again, at a slower rate than when cinchonidine is present in solution. In fact, CO cannot be completely removed in the absence of cinchonidine even after O_2 bubbling for 3.0–4.0 h, especially in the case of the higher initial CO

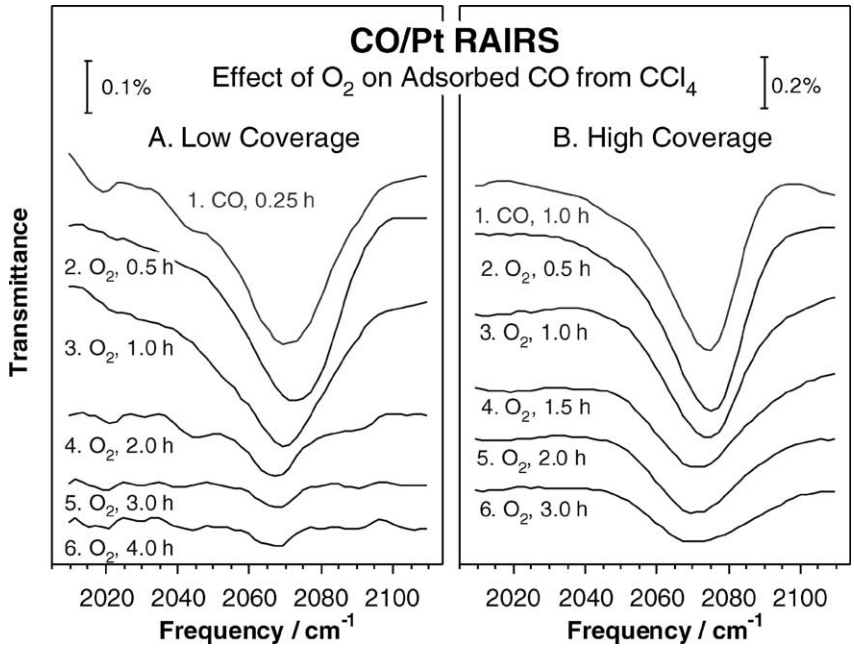

Fig. 10. RAIRS data illustrating the effect of O_2 on CO adsorbed from pure CCl_4 at two different initial CO coverages. The coadsorption of O_2 causes the removal of adsorbed CO, the same as in the experiment reported in Fig. 9. However, the CO removal is faster and more complete in the presence of cinchonidine in the solution.

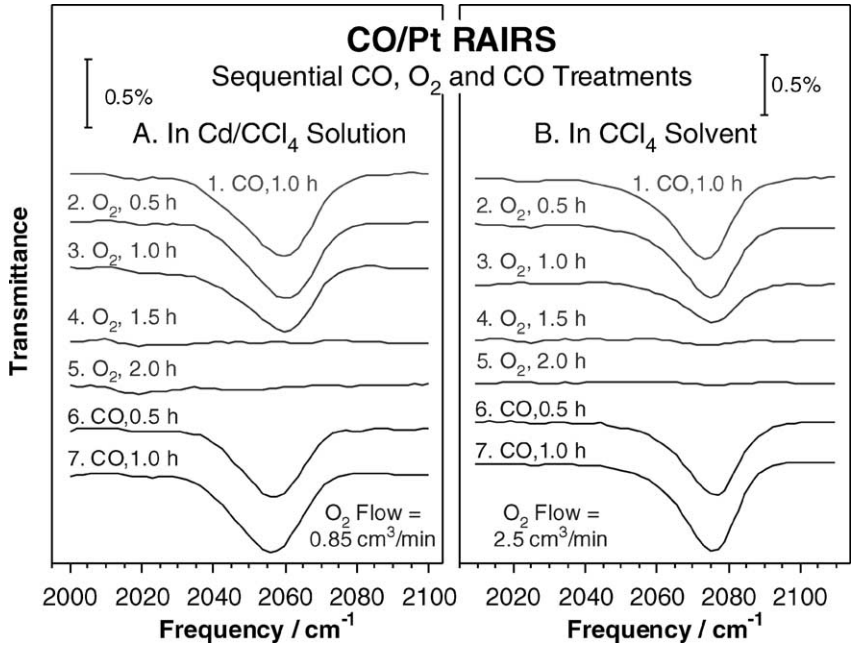

Fig. 11. RAIRS results from gas-switching experiments from CO to O_2 and back to CO. Two sets of data are shown here, one carried out with a cinchonidine solution (A), and the other in the pure CCl_4 solvent (B). As shown before, O_2 removes the surface-adsorbed CO in both cases (a high O_2 flux was used in the case of pure CCl_4 to accelerate this process), but without any appreciable cinchonidine uptake in the first case. In addition, this figure shows that CO can be readsorbed afterward, presumably by removing some surface oxygen via a CO(ads) + O(ads) reaction. No cinchonidine uptake takes place during this process either.

coverage. This is to be contrasted with the easy removal of all the surface CO after only 1.5 h of O_2 bubbling in the presence of cinchonidine (Fig. 9). The data in Figs. 9 and 10 further confirm that O_2 can indeed remove adsorbed CO and that this removal can be facilitated by the presence of a small amount of cinchonidine in solution.

It is also of interest to reassert that the removal of CO in the presence of O_2 does not induce any significant cinchonidine adsorption (Fig. 9), in clear contrast with the case of the removal of CO by H_2 (Fig. 6). To further understand this point, CO titration experiments were carried out after the CO–O_2 treatment sequence both in the presence and in

the absence of cinchonidine (Fig. 11). The final CO IR intensity in both cases (with and without cinchonidine) was about 30–40% that on a clean, metallic Pt surface, indicating that the exchange of O_2 by CO in solution does lead to the opening of some new Pt sites on the surface, but only for CO, not cinchonidine, adsorption. This observation is consistent with the titration experiment shown in the third trace of Fig. 5. All these data show that switching between CO and O_2 exposures leads to an alternation between carbon monoxide and oxygen covering of approximately half of the platinum surface sites. However, at no point during these cycles do new adsorption sites for cinchonidine open up; only hydrogen treatments can reduce the Pt surface (Fig. 5) and induce such increase in cinchonidine adsorption (Fig. 9).

4. Discussion

As mentioned in Section 1, the performance of cinchona-modified platinum for enantioselective hydrogenation catalysis is quite sensitive to a number of parameters, among them the presence of gases in the solution of the reactant and modifier. It has been the objective of this study to shed some light on the effect of different dissolved gases on the adsorption of cinchonidine from solution onto platinum surfaces and on how these effects translate into the cinchonidine modifying behavior in catalysis.

4.1. Facilitating effect of H_2 on cinchonidine adsorption

In the case of hydrogenation reactions, as in the cinchona/Pt system studied here, H_2 is one of the main reactants, and is thereby always present in the solution. However, results from the present study, as well as from others [20], clearly indicate that H_2 also plays a second role in this catalysis, namely, it helps condition the surface of the Pt catalyst to facilitate the adsorption of the chiral modifier. It was found from our studies that if the Pt surface is exposed to cinchonidine solutions either in the absence of any bubbling of gases or after saturation of the solution with Ar, N_2, O_2, air, or CO_2, cinchonidine adsorption is barely detected (Fig. 2). On the other hand, once the surface is treated with H_2, extensive cinchonidine uptake is observed (Figs. 3 and 4). Even if the surface is not previously cleaned by oxidation–reduction cycles, as typically done in these studies, or if it is exposed to a strong inhibitor such as CO (Fig. 6), H_2 can still incite the adsorption of cinchonidine, albeit at a lower rate in the latter case. It has been suggested that the reason why cinchona-modified catalysts may not perform well in the absence of hydrogen treatments is that under those conditions the reactant (ethyl pyruvate, for instance) undergoes aldol condensation and polymerizes on the surface [18]. Our studies clearly indicate that, regardless of the validity of that argument, hydrogen also affects the adsorption of the cinchona modifier directly.

The CO titration experiments reported in Fig. 5 also show that exposure of the surface to O_2 leads to blocking of adsorption sites for cinchonidine, and that the activity of the oxygen-treated surfaces can be restored only by subsequent hydrogen treatments (Fig. 3). It seems that cinchonidine adsorption takes place only on clean, metallic Pt sites. In addition, it can also be postulated that, without the presence of dissolved H_2 in solution, the Pt surface may be at least partially oxidized [47–51] and/or covered by surface contaminants [47,52,53]. Nevertheless, the availability of some Pt sites cannot be excluded in that case, as evident by the fact that CO can still adsorb on such surfaces (Fig. 5). It could be argued that it may be more difficult for cinchonidine to adsorb on the surface, because that molecule is quite bulky and requires large Pt surface ensembles [10,27,34,35,54]. The adsorption sites available on the partially oxidized surface evidenced by the CO adsorption may consist mainly of isolated Pt atoms.

The difference in behavior between CO and cinchonidine adsorption deserves a closer look. As stated above, our suggestion is that cinchonidine adsorption is more demanding because it requires larger ensembles of surface Pt metal atoms. CO, on the other hand, can adsorb in small surface sites in between atomic oxygen adsorbates. This latter idea is in fact supported by the low C–O stretching frequencies observed for carbon monoxide adsorbed on the oxygen-treated surfaces (middle trace in Fig. 5), since similar IR low frequencies are typically associated with isolated molecules at low coverages [55,56]. Co-adsorption of CO on oxygen-covered metal surfaces is not surprising, and is seen, for instance, on the (2×2)-O layer that forms on Pt(111) after O_2 saturation [56,57]. The idea of adsorbed oxygen blocking adsorption sites and breaking large metallic Pt surface ensembles but leaving isolated sites open for CO adsorption helps explain why adsorption of only a small amount of O can selectively hinder the adsorption of cinchonidine. The idea could then be advanced that H_2 efficiently removes the atomic oxygen deposited on the surface upon exposures to O_2 (and also any other surface impurities), freeing larger patches of Pt sites, and thus facilitating the adsorption of cinchonidine. On the other hand, although CO can certainly remove some adsorbed oxygen, it can also simultaneously block surface sites, making them unavailable for cinchonidine adsorption (more on this later).

A couple of additional issues related to the availability of adsorption sites for cinchonidine and CO on the Pt surface at the different stages of our experiments need to be briefly mentioned here. In particular, it is worth noting that significant amounts of CO, up to close to half-saturation, can be adsorbed on surfaces where no cinchonidine uptake is possible, in particular when no hydrogen pretreatments are used (Fig. 5). Given that a polycrystalline Pt disk was used in our experiments, this could be interpreted as being the consequence of the availability of different crystallographic facets on the surface. It may be that cinchonidine adsorbs only on wide flat surfaces terraces, while CO can bind to many

other sites in rougher planes with steps, kinks, and other defects. Indeed, enantioselectivity on cinchona-modified catalysis has been reported to depend strongly on the particle size and dispersion of the metal [28,58–60]. Nevertheless, the large amounts of both cinchonidine and CO that adsorb on the surface, together with the changes in vibrational frequencies seen for the C–O stretch when in the presence versus in the absence of cinchonidine observed in our experiments (compare, for instance, the spectra in Figs. 6 and 8), argue against this explanation. In addition, our work shows that even after saturation of the Pt surface with cinchonidine, there are still empty sites open for CO readsorption (bottom two traces in Fig. 6). In fact, the CO uptake on surfaces saturated with cinchonidine leads to a similar surface concentration as in the case where CO is adsorbed first to block the adsorption sites for cinchonidine (top two traces in Fig. 6), and to almost the same surface coverage as when starting with fresh pure CCl_4 solutions (Fig. 5). We interpret these results as a consequence of the fact that the cinchonidine surface layer resulting from exposure of the Pt surface to cinchonidine/CCl_4 solutions is not compact [29,61]. It may be that the same sites manifested by the CO titration experiment in Fig. 6 are available for adsorption of the reactants, H_2 and α-ketoester, during catalysis.

In terms of the time dependence of the response of the cinchonidine/Pt to H_2 treatments, our results in Fig. 4 show that significant cinchonidine adsorption starts after as little as 5 min of H_2 bubbling, and reaches a maximum after 30 min of this treatment. It should be noted that no adsorbates could be clearly identified by IR spectroscopy before the hydrogen treatment. This is not to say that at that stage of our experiments the Pt surface is clean, only that any adsorbed species are invisible to our IR spectroscopic characterization technique. In fact, we believe that the hydrogen treatment is needed to remove adsorbed oxygen or other contaminants (and reduce a PtO_x film if present on the surface). In any case, it is clear that the adsorption of cinchonidine on Pt in the presence of H_2 does require some time. On the other hand, it is also noted that the cinchonidine peaks decrease after long H_2 bubbling, for exposures longer than 30–45 min. It could be thought that this change may be due to poisoning of the Pt surface, but such an idea can be ruled out because (1) switching from H_2 to Ar, N_2, O_2, air, or CO_2 for 2.0–3.0 h does not cause any loss of cinchonidine adsorption (Fig. 3), and (2) replacement of the used cinchonidine solution with a fresh one regenerates the surface layer even if no additional special cleaning of the surface is performed (Fig. 4). Instead, the gradual decrease in IR signal for cinchonidine with H_2 exposure is likely related to the loss of the adsorbed modifier from the Pt catalysts. Because of mass transfer constraints within our experimental setup, our measurements do not provide accurate kinetic information on either the initial cleaning of the surface or the subsequent reduction of the cinchonidine. Nevertheless, we believe that those limitations do not modify the qualitative conclusions reported here.

The gradual hydrogenation of cinchonidine has been independently verified in the past for similar systems by analysis of the liquid solution with thin-layer chromatography [29], UV–vis spectroscopy ESI-MS [43,44], and GC-MS [45]. Our direct in situ spectroscopic evidence for the time-dependent disappearance of cinchonidine on the surface of the Pt catalyst complements previous results based either on the detection of the hydrogenated species in solution or on measurements of enantioselectivities during reaction. To circumvent the gradual loss of chiral modifier during catalysis, fresh cinchonidine can be added either before each catalytic process cycle [62] or during the course of reaction [34,35,63]. In this study, addition of a fresh cinchonidine solution and extra H_2 bubbling after the decrease of cinchonidine IR peaks led to restoration of the cinchonidine-saturated surface. Our evidence for the in situ regeneration of surface cinchonidine species visualizes the remediation method used in catalysis from a surface chemistry perspective.

4.2. Poisoning effect of CO

It has been previously noted that CO adsorption on the surface may affect the enantioselective hydrogenation of α-ketoesters by cinchona-modified platinum catalysts. For example, the reported decrease in activity and enantioselectivity for the hydrogenation of ethyl pyruvate on catalysts containing anchored silicium organic moieties has been ascribed to poisoning by chemisorbed carbon monoxide [64]. In another study, the reported decrease in ethyl pyruvate hydrogenation rate by addition of formic acid to the reaction mixture has been explained by surface poisoning resulting from decomposition to CO [65]. Finally, the drastic loss of activity for ethyl pyruvate hydrogenation in supercritical CO_2 may be due to the formation of CO via the reverse of the water gas-shift reaction, that is, by the conversion of CO_2 and H_2 to CO and H_2O [36–38]. Our in situ spectroscopic experiments give credence to those arguments by indicating that, indeed, CO adsorbs quite strongly on Pt, and significantly retards the H_2-assisted cinchonidine adsorption (Fig. 6).

Additional experiments were carried out in our laboratory to further explore the poisoning behavior of formic acid. It was found that when adding as little as 0.01% of formic acid to the liquid solution in our IR cell, detectable amounts of CO could be seen by IR spectroscopy on the Pt sample (data not shown). This indicates a facile decomposition of formic acid to carbon monoxide under our experimental conditions. Similar behavior was seen with formaldehyde. On the other hand, no CO production was ever observed in our experiments with H_2 and CO_2, so no direct evidence for the possibility of a reverse gas shift during catalysis was obtained. Nevertheless, that reaction has been reported on Pt/Al_2O_3 catalysts at 40 °C [36,66].

It is worth noting that, as shown in Fig. 6, adsorbed CO can eventually be removed by H_2. Past catalytic studies also

indicated that both activity and enantioselectivity can be restored on CO-deactivated cinchona-modified Pt catalysts after switching the solvent from supercritical CO_2 to ethane in the presence of H_2 [37]. To better understand the removal of adsorbed CO by dissolved H_2, it is useful to focus on two key differences between Figs. 6 and 8. First, it is seen that while the initial CO IR peak develops at 2060 cm^{-1} when cinchonidine is present in solution (Fig. 6), it appears at about 2067 and 2076 cm^{-1} for lower and higher CO coverages, respectively, in the absence of cinchonidine at the CCl_4/Pt interface (Fig. 8). This strongly suggests that the adsorption of even a small amount of cinchonidine affects the interaction of CO with the Pt surface. The frequency changes of the CO IR peak are often linked to the electron donor or acceptor nature of the co-adsorbate [46,47], to the CO surface coverage, and/or to the potentials applied in electrochemical settings [67]. Adsorbed H_2, benzene, and pyridine increase the electron density of the Pt surface atoms and, accordingly, increase the extent of the backdonation of electrons from the metal *d* orbitals to the $2\pi^*$ anti-bonding orbital of CO, forcing the stretching frequency of CO to red shift [46,47]. The adsorption of cinchonidine, either by π interaction with the Pt surface or by donation of electrons from the lone electron pair in the nitrogen of the quinoline ring to the metal, may also cause a red shift in the CO IR peak position [38]. Nevertheless, some of the red shift in the C–O stretching frequency on co-adsorption with cinchonidine may also be associated with differences in the distribution of the adsorbates on the surface. It is possible for CO molecules to be distributed in isolated platinum sites in between adsorbed cinchonidine molecules; as mentioned before, individual CO adsorbates display lower IR frequencies than when adsorbed in islands or at higher coverages [55,56].

A second difference between the cases in Figs. 6 and 8 is the further red shift of 17 cm^{-1} (and the obvious reduction in CO surface coverage) observed during the H_2 treatment in the presence of cinchonidine. This red shift is less extensive ($\Delta\nu \leqslant 10$ cm^{-1}) in the absence of cinchonidine, and the CO concentration on the surface does not obviously decrease in that case either. The disparity between the two sets of data can easily be ascribed to the role played by cinchonidine co-adsorption with CO. H_2-induced CO displacement has been reported on Ni and Pt surfaces in vacuum [68–70]. The effectiveness of this process has been reported to depend on a number of factors, including the nature and temperature of substrate, the concentrations of H_2 and CO, and the time on stream. In particular, the CO displacement rate increases with both substrate temperature and H_2 pressure, and is more rapid for the weakly bound CO than for its more tightly bound form [68–70]. Our results in Fig. 8 show that, in the absence of cinchonidine, H_2-induced CO displacement does not readily occur under our experimental conditions even for submonolayer initial CO coverages, but this may be easily explained by the relatively low concentrations of H_2 in the liquid phase. On the other hand, a synergistic effect between H_2 and cinchonidine toward the displacement of CO is possible. The Pt–CO bond may be substantially weakened in the presence of even a small amount of co-adsorbed cinchonidine, perhaps because of the electron-donating effect of the adsorbed modifier [70]. Also interesting is the fact that, after an induction period of close to 2.0 h of exposure of the CO-saturated surface to hydrogen (in the presence of cinchonidine), the displacement of the adsorbed CO by cinchonidine is relatively fast (Fig. 7). It could be argued that a critical extent of CO desorption needs to be reached before cinchonidine can adsorb on the surface, perhaps because the high mobility of remaining adsorbed CO leads to the fast blocking of the initial sites obtained by H_2-induced CO desorption (and to a less dense but homogeneous CO surface layer). Only after a sufficient number of CO molecules have been removed from the surface it is possible to find Pt atomic ensembles large enough for cinchonidine adsorption. At that point, cinchonidine may, in fact, assist in the displacement of the last adsorbed carbon monoxide.

4.3. CO removal in the presence of O_2 and cinchonidine

Our experiments indicate that, in contrast to the case of H_2, adsorbed CO can be removed from the surface by O_2 dissolved in CCl_4 solutions in both the presence and the absence of cinchonidine (Figs. 9 and 10). Control experiments also indicate that N_2 cannot remove the adsorbed CO in either case. Therefore, the CO removal mechanism in the presence of O_2 most likely involves a surface oxidation mechanism. It is well known that O_2 dissociates on Pt sites to form atomic surface oxygen, and reacts with adsorbed CO to form CO_2 [48,49]. The fact that CO can also be adsorbed on oxygen-treated surfaces (Figs. 5 and 11) supports this idea, because if one gas were to just displace the other from the surface, the process should not be reversible, but end with saturation of the surface with the more strongly bonded adsorbate. In addition, the surface oxidation of CO is slow at room temperature [49]; our experiments with O_2 on CO precovered surface and without cinchonidine point to this fact (Fig. 10). On the other hand, the CO removal rate is accelerated in the presence of cinchonidine (Fig. 9), indicating the facilitating role of cinchonidine toward CO removal, the same as with H_2. Note that indeed a small amount of cinchonidine is adsorbed on the surface throughout the sequence where CO is displaced by either H_2 or O_2 (Figs. 6 and 9).

The behavior seen with CO–H_2 and CO–O_2 switching experiments suggests that in both cases the displacement of the adsorbed CO by the second adsorbate may be somewhat reversible unless the vacated surface sites are irreversibly blocked by cinchonidine. In fact, that argument may fully account for the displacement of CO by H_2, but does not entirely explain the effect seen with O_2. For the latter case, it is of interest to note that as O_2 removes the CO on surface, it does not facilitate an increase in the adsorption of cinchonidine (Fig. 9). This contrasts with the behavior seen with H_2, where CO displacement and cinchonidine adsorption take

place concurrently (Fig. 6). On the other hand, Figs. 5, 6, and 9 show that exposure of the Pt surface to CO in the presence of cinchonidine/CCl_4 solutions leads only to a partial uptake of the carbon monoxide on the surface, up to less than half of saturation. It appears that the Pt surface at this stage is partially blocked, perhaps by oxygen from air dissolved in the CCl_4 solvent, small amounts of cinchonidine, and/or other contaminants. The sites left on surfaces not treated with hydrogen after exposure to the cinchonidine/CCl_4 solution are not big enough for the adsorption of additional cinchonidine, but can still adsorb CO. As CO molecules are then removed by O_2, oxygen atoms are left on the surface in their place, and that keeps the open surface sites still small enough for any significant cinchonidine uptake. It is even possible for two different sites to exist on the surface with different strengths toward O_2 adsorption, but, most likely, cinchonidine affects the rate of CO displacement via an electronic interaction that weakens the Pt–CO bond. In any case, only H_2 treatments remove enough oxygen surface atoms to allow for the adsorption of cinchonidine and, presumably, to promote enantioselective hydrogenation catalysis.

One final note of caution. The studies reported here were carried out with carbon tetrachloride solutions, a choice made because of experimental considerations. However, CCl_4 is not the preferred solvent for the chiral cinchona modification of platinum catalysts to improve their activity and enantioselectivity [62,71]. In fact, vast differences in catalyst performance have been reported with various solvents. This may cast some doubts on the validity of our conclusions to real catalytic systems. Nevertheless, we believe that in terms of the effect of dissolved gases on the adsorption of cinchonidine, qualitatively similar results are expected regardless of solvent. In any case, further work is underway in our laboratory to better address the role of the nature of the solvent on the performance of these systems [42].

5. Conclusions

In these studies, the role of dissolved gases in the adsorption of cinchonidine from liquid solutions onto Pt surfaces was characterized by in situ RAIRS. It was found that the O_2 present in most cinchonidine solutions from dissolved air [51] blocks the surface toward any cinchonidine uptake, presumably via its dissociation to atomic surface oxygen atoms (and maybe by partial oxidation of the platinum surface). Exposures of the platinum surface to solutions bubbled with Ar, N_2, O_2, air, or CO_2 do not help with the adsorption of cinchonidine either. H_2 dissolved in solution, on the other hand, does facilitate the adsorption of cinchonidine in a significant way, perhaps because it helps reduce the metal surface and remove any surface contaminants. However, the adsorbed cinchonidine layer that builds up in that case is not compact, and still leaves unoccupied Pt sites available for the adsorption of smaller molecules such as CO, and perhaps the reactant during catalysis. The adsorption of cinchonidine from CCl_4 solutions is also highly irreversible: adsorbed cinchonidine can hardly be displaced by any of the gases studied here, and cannot be easily desorbed by the pure CCl_4 solvent either. On the other hand, that cinchonidine can be slowly removed from the surface by dissolved H_2, presumably via its hydrogenation, and regenerated by exposure to fresh cinchonidine solutions.

A number of empirical observations from catalytic studies on the enantioselective hydrogenation of ethyl pyruvate using cinchona-modified platinum have been ascribed to a poisoning effect of carbon monoxide on the surface of the catalyst. In the present investigation it was found that CO is a strong inhibitor for cinchonidine adsorption. Nevertheless, it was also seen that adsorbed CO can be slowly removed by H_2 dissolved in cinchonidine solutions. There is a synergistic effect between cinchonidine and H_2 in terms of CO displacement, since H_2 alone is not enough to remove the adsorbed carbon monoxide under our experimental conditions. CO can also be removed by dissolved O_2, most likely via a reaction to produce CO_2, but that process is not accompanied by subsequent cinchonidine adsorption. These results underline the key role played by H_2 in conditioning the working Pt catalysts to facilitate the adsorption of cinchona modifiers from solution onto active Pt sites.

Acknowledgments

Financial support for this work was provided by the Petroleum Research Fund of the American Chemical Society and by the National Science Foundation. Additional funds were provided by the Merck Research Laboratories.

References

[1] R. Noyori, Angew. Chem., Int. Ed. Engl. 41 (2002) 2008.
[2] A.N. Collins, G.N. Sheldrake, J. Crosby, Chirality in Industry: The Commercial Manufacture and Applications of Optically Active Compounds, Wiley, New York, 1995.
[3] A. Baiker, H.U. Blaser, in: G. Ertl, H. Knözinger, J. Weitkamp (Eds.), Handbook of Heterogeneous Catalysis, Vol. 4, VCH, Weinheim, 1997, p. 2422.
[4] Y. Izumi, Adv. Catal. 32 (1983) 215.
[5] T. Osawa, T. Harada, A. Tai, Catal. Today 37 (1997) 465.
[6] G. Webb, P.B. Wells, Catal. Today 12 (1992) 319.
[7] R.L. Augustine, S.K. Tanielyan, L.K. Doyle, Tetrahedron: Asymmetry 4 (1993) 1803.
[8] J. Wang, Y. Sun, C. Leblond, R.N. Landau, D.G. Blackmond, J. Catal. 161 (1996) 752.
[9] J.L. Margitfalvi, M. Hegedüs, E. Tfirst, in: J.W. Hightower, W.N. Delgass, E. Iglesia, A.T. Bell (Eds.), Proceedings of the 11th International Congress on Catalysis, 40th Anniversary, Baltimore, MD, USA, June 30–July 5, 1996 (Studies in Surface Science and Catalysis, Vol. 101, Part A), Elsevier, Amsterdam, 1996, p. 241.
[10] A. Baiker, J. Mol. Catal. A 115 (1997) 473.
[11] H.-U. Blaser, H.-P. Jalett, M. Müller, M. Studer, Catal. Today 37 (1997) 441.

[12] B. Török, K. Balázsik, K. Felföldi, M. Bartók, Ultrason. Sonochem. 8 (2001) 191.
[13] R. Raval, CATTECH 5 (2001) 12.
[14] K.E. Simons, P.A. Meheux, S.P. Griffiths, I.M. Sutherland, P. Johnston, P.B. Wells, A.F. Carley, M.K. Rajumon, M.W. Roberts, A. Ibbotson, Recl. Trav. Chim. Pays-Bas 113 (1994) 465.
[15] A.F. Carley, M.K. Rajumon, M.W. Roberts, P.B. Wells, J. Chem. Soc., Faraday Trans. 91 (1995) 2167.
[16] T. Evans, A.P. Woodhead, A. Gutiérrez-Sosa, G. Thornton, T.J. Hall, A.A. Davis, N.A. Young, P.B. Wells, R.J. Oldman, O. Plashkevych, O. Vahtras, H. Ågren, V. Carravetta, Surf. Sci. 436 (1999) L691.
[17] J.M. Bonello, R.M. Lambert, Surf. Sci. 498 (2002) 212.
[18] J.M. Bonello, E.C.H. Sykes, R. Lindsay, F.J. Williams, A.K. Santra, R.M. Lambert, Surf. Sci. 482–485 (2001) 207.
[19] D. Ferri, T. Bürgi, A. Baiker, J. Catal. 210 (2002) 160.
[20] D. Ferri, T. Bürgi, J. Am. Chem. Soc. 123 (2001) 12074.
[21] D. Ferri, T. Bürgi, A. Baiker, Chem. Commun. (2001) 1172.
[22] J. Kubota, F. Zaera, J. Am. Chem. Soc. 123 (2001) 11115.
[23] W. Chu, R.J. LeBlanc, C.T. Williams, Catal. Commun. 3 (2002) 547.
[24] G.A. Somorjai, Surf. Sci. 335 (1995) 10.
[25] F. Zaera, Surf. Sci. 500 (2002) 947.
[26] Y. Orito, S. Imai, S. Niwa, Nippon Kagaku Kaishi (1980) 670.
[27] H.U. Blaser, H.P. Jalett, D.M. Monti, J.T. Wehrli, Appl. Catal. 52 (1989) 19.
[28] T. Mallat, S. Frauchiger, P.J. Kooyman, M. Schürch, A. Baiker, Catal. Lett. 63 (1999) 121.
[29] I.M. Sutherland, A. Ibbotson, R.B. Moyes, P.B. Wells, J. Catal. 125 (1990) 77.
[30] B. Minder, T. Mallat, P. Skrabal, A. Baiker, Catal. Lett. 29 (1994) 115.
[31] R.L. Augustine, S.K. Tanielyan, J. Mol. Catal. A 118 (1997) 79.
[32] R.L. Augustine, S.K. Tanielyan, J. Mol. Catal. A 112 (1996) 93.
[33] M. Bartók, G. Szöllösi, K. Balázsik, T. Bartók, J. Mol. Catal. A 177 (2002) 299.
[34] C. LeBlond, J. Wang, J. Liu, A.T. Andrews, Y.K. Sun, J. Am. Chem. Soc. 121 (1999) 4920.
[35] C. LeBlond, J. Wang, A.T. Andrews, Y.K. Sun, Top. Catal. 13 (2000) 169.
[36] B. Minder, T. Mallat, K.H. Pickel, K. Steiner, A. Baiker, Catal. Lett. 34 (1995) 1.
[37] R. Wandeler, N. Kunzle, M.S. Schneider, T. Mallat, A. Baiker, Chem. Commun. (2001) 673.
[38] X. You, X. Li, S. Xiang, S. Zhang, Q. Xin, X. Li, C. Li, in: A. Corma, F.V. Melo, S. Mendioroz, J.L.G. Fierro (Eds.), Proceedings of the 12th International Congress on Catalysis, 2000 (Studies in Surface Science and Catalysis, Vol. 130, Part D), Amsterdam, Elsevier, 2000, p. 3375.
[39] F. Zaera, Acc. Chem. Res. 35 (2002) 129.
[40] F. Zaera, Int. Rev. Phys. Chem. 21 (2002) 433.
[41] J. Kubota, Z. Ma, F. Zaera, Langmuir 19 (2003) 3371.
[42] Z. Ma, J. Kubota, F. Zaera, 2003, in preparation.
[43] B. Török, K. Balázsik, M. Török, G. Szöllösi, M. Bartók, Ultrason. Sonochem. 7 (2000) 151.
[44] M. Bartók, K. Balázsik, G. Szöllösi, T. Bartók, J. Catal. 205 (2002) 168.
[45] V. Morawsky, U. Prüße, L. Witte, K.-D. Vorlop, Catal. Commun. 1 (2000) 15.
[46] M. Primet, J.M. Basset, M.V. Mathieu, M. Prettre, J. Catal. 29 (1973) 213.
[47] D. Ferri, T. Bürgi, A. Baiker, J. Phys. Chem. B 105 (2001) 3187.
[48] T. Engel, G. Ertl, Adv. Catal. 28 (1979) 1.
[49] G. Ertl, J. Mol. Catal. A 182–183 (2002) 5.
[50] T. Mallat, M. Bodmer, A. Baiker, Catal. Lett. 44 (1997) 95.
[51] P.B. Wells, K.E. Simons, J.A. Slipszenko, S.P. Griffiths, D.F. Ewing, J. Mol. Catal. A 146 (1999) 159.
[52] B. Minder, T. Mallat, A. Baiker, G. Wang, T. Heinz, A. Pfaltz, J. Catal. 154 (1995) 371.
[53] T. Mallat, Z. Bodnar, B. Minder, K. Borszeky, A. Baiker, J. Catal. 168 (1997) 183.
[54] G. Bond, K.E. Simons, A. Ibbotson, P.B. Wells, D.A. Whan, Catal. Today 12 (1992) 421.
[55] R.A. Shigeishi, D.A. King, Surf. Sci. 58 (1976) 379.
[56] F. Zaera, J. Liu, M. Xu, J. Chem. Phys. 106 (1997) 4204.
[57] A. Szabo, M. Kiskinova, J.T. Yates Jr., J. Chem. Phys. 90 (1989) 4604.
[58] J.T. Wehrli, A. Baiker, D.M. Monti, H.U. Blaser, J. Mol. Catal. 61 (1990) 207.
[59] H.U. Blaser, H.P. Jalett, D.M. Monti, A. Baiker, J.T. Wehrli, Structure–activity and selectivity relationships in heterogeneous catalysis, in: R.K. Grasselli, A.W. Sleight (Eds.), Proceedings of the ACS Symposium on Structure–Activity Relationships in Heterogeneous Catalysis, Boston, MA, USA, April 22–27, 1990 (Studies in Surface Science and Catalysis Series, Vol. 67), Elsevier, Amsterdam, 1991, p. 147.
[60] Y. Nitta, T. Kubota, Y. Okamoto, Bull. Chem. Soc. Jpn. 74 (2001) 2161.
[61] H.U. Blaser, M. Garland, H.P. Jallet, J. Catal. 144 (1993) 569.
[62] J.T. Wehrli, A. Baiker, D.M. Monti, H.U. Blaser, H.P. Jalett, J. Mol. Catal. 57 (1989) 245.
[63] N. Kunzle, R. Hess, T. Mallat, A. Baiker, J. Catal. 186 (1999) 239.
[64] J.L. Margitfalvi, E. Tálas, Appl. Catal. A 182 (1999) 65.
[65] H.U. Blaser, H.P. Jalett, J. Wiehl, J. Mol. Catal. 68 (1991) 215.
[66] D. Ferri, T. Bürgi, A. Baiker, Phys. Chem. Chem. Phys. 4 (2002) 2667.
[67] S.M. Stole, D.D. Popenoe, M.D. Porter, in: H.D. Abruña (Ed.), Electrochemical Interfaces: Modern Techniques for In-Situ Interface Characterization, VCH, New York, 1991, p. 339.
[68] S. Shen, F. Zaera, D.A. Fischer, J.L. Gland, J. Chem. Phys. 89 (1988) 590.
[69] J.L. Gland, S. Shen, F. Zaera, D.A. Fischer, J. Vac. Sci. Technol. A 6 (1988) 2426.
[70] J.L. Gland, D.A. Fischer, S. Shen, F. Zaera, J. Am. Chem. Soc. 112 (1990) 5695.
[71] P.J. Collier, T.J. Hall, J.A. Iggo, P. Johnston, J.A. Slipszenko, P.B. Wells, R. Whyman, Chem. Commun. (1998) 1451.